Organometallics 1993, 12, 704–711

(Fluoroalkyl)phosphine Hydride Complexes of Iridium. Synthesis and Structures of $(dfepe)_2IrH$ and $(dfepe)_2Ir_2(H)(\mu\text{-}H)_2(\mu\text{-}O_3SCF_3)$

R. Chris Schnabel and Dean M. Roddick*

Chemistry Department, Box 3838, University of Wyoming, Laramie, Wyoming 82071

Received October 13, 1992

The synthesis and characterization of a series of (fluoroalkyl)phosphine complexes of iridium are described. Treatment of $[(cod)Ir(thf)_2]OTf$ with $(C_2F_5)_2PCH_2CH_2P(C_2F_5)_2$ ("dfepe") affords $[(dfepe)Ir(cod)]OTf$ (**1**), which serves as a versatile precursor to a variety of (dfepe)Ir complexes. Reaction of **1** with acetonitrile yields $[(dfepe)Ir(MeCN)_2]OTf$ (**2**). In the presence of free dfepe, the hydrogenolysis of **1** affords the cationic dihydride *cis*-$[(dfepe)_2Ir(H)_2]OTf$ (**3**), which is readily deprotonated by weak bases to give the structurally characterized neutral hydride $(dfepe)_2IrH$ (**4**). Protonation of **4** to regenerate $(dfepe)_2Ir(H)_2^+$ is effected only by the strong acid HOTf. Although **4** is stabile toward MeCN, **3** readily loses one dfepe ligand in MeCN solvent to give $[(dfepe)Ir(MeCN)(H)_2]OTf$ (**7**). Treatment of **4** with CO, however, results in the clean displacement of one dfepe ligand to form $(dfepe)Ir(CO)_2H$ (**6**). Hydrogenolysis of **1** in the absence of dfepe or donor solvents leads to the formation of the sparingly soluble symmetrical dimeric Ir(III) polyhydride $[(dfepe)Ir(H)(\mu\text{-}H)(OTf)]_2$ (**8**). Like **3**, **8** is highly acidic and readily deprotonates to form the asymmetric dimer $(dfepe)_2Ir_2(H)(\mu\text{-}H)_2(\mu\text{-}O_3SCF_3)$ (**9**). The presence of a bridging triflate ligand in **9** has been confirmed by X-ray crystallography. Attempts to further deprotonate **9** to form the parent $[(dfepe)Ir(\mu\text{-}H)]_2$ have thus far been unsuccessful. Crystal data for **4**: orthorhombic, $P2_12_12_1$, with $a = 11.706(4)$ Å, $b = 16.449(5)$ Å, $c = 18.497(5)$ Å, $V = 3572.5(5)$ Å^3, $Z = 4$, $R_F = 6.45\%$, and $R_{wF} = 6.65\%$. Crystal data for **9**: monoclinic, $P2_1/n$, with $a = 10.915(3)$ Å, $b = 19.967(4)$ Å, $c = 19.898(5)$ Å, $\beta = 102.58(2)°$, $V = 4232(2)$ Å^3, $Z = 4$, $R_F = 6.25\%$, and $R_{wF} = 8.43\%$.

Introduction

Hydride complexes of the cobalt triad play an important role in a number of important catalytic processes involving hydrogen atom transfer.[1-3] Well-studied rhodium and iridium systems include the simple phosphine complexes $(Ph_3P)_4RhH$ and $(^iPr_3P)_2IrH_5$,[4] the mixed carbonyl phosphine complexes $(Ph_3P)_2M(CO)H$, and the cationic solvates $(R_3P)_2IrH_2(solv)_2^+$.[5] The activity of these compounds generally relies on the facile oxidative addition of H_2 or substrate X–H bonds to an unsaturated electron-rich M(I) center.[6] With the notable exception of $(CO)_4CoH$,[7] comparatively little is known about the corresponding chemistry of electron-poor polycarbonyl analogues. Unlike the first-row congener $(CO)_4CoH$, analogous complexes of rhodium and iridium are unstable with respect to cluster formation.[8] It is particularly intriguing that carbonylation catalyst systems such as $Rh_6(CO)_{16}$ and $Rh_4(CO)_{12}$, which operate under extreme pressure and temperature conditions, likely involve mononuclear carbonyls as the active species.[2,9] Monomeric fluorophosphine derivatives $(F_3P)_4MH$ (M = Co, Rh, Ir) which approximate the electronic properties of $(CO)_4MH$ systems are known, but these complexes have limited thermal stability.[10]

For several years we have been exploring the applications of the π-acid (fluoroalkyl)phosphine chelate $(C_2F_5)_2PCH_2CH_2P(C_2F_5)_2$ ("dfepe") to a variety of problems in coordination chemistry.[11] Unlike fluorophosphine ligands, fluoroalkylphosphines are stabilized toward P–X bond cleavage and exert considerably more steric influence and thus are more suited for the design of coordinatively unsaturated electrophilic acceptor complexes. Following our initial studies of the iridium and rhodium (fluoroalkyl)phosphine dimeric halides $[(dfepe)M(\mu\text{-}Cl)]_2$,[12] we have begun to examine synthetic routes to group IX systems which incorporate potentially reactive hydride ligands. In this paper we present the synthesis and properties of the bis-chelate hydride complexes $(dfepe)_2IrH$ and *cis*-$[(dfepe)_2IrH_2]^+OTf^-$ as well as the synthesis and

---

[1] (a) Jardine, F. H. In *Chemistry of the Platinum Group Metals*; Hartley, F. R., Ed.; Elsevier: New York, 1991; Chapter 13. (b) Koga, N.; Morokuma, K. In *Transition Metal Hydrides*; Dedieu, A., Ed.; VCH: New York, 1991; Chapter 6. (c) Catalytic Transition Metal Hydrides. *Ann. N.Y. Acad. Sci.* **1983**, *415*.

[2] Dickson, R. S. *Homogeneous Catalysis with Compounds of Rhodium and Iridium*; D. Reidel: Dordrecht, Holland, 1985.

[3] *Homogeneous Catalysis with Metal Phosphine Complexes*; Pignolet, L. H., Ed.; Plenum: New York, 1983.

[4] (a) Faller, J. W.; Smart, C. J. *Organometallics* **1989**, *8*, 602. (b) Cameron, C. J.; Felkin, H.; Fillebeen-Khan, T.; Forrow, N. J.; Guittet, E. *J. Chem. Soc., Chem. Commun.* **1986**, 801.

[5] (a) Crabtree, R. H.; Mellea, M. F.; Mihelcic, J. M.; Quirk, J. M. *J. Am. Chem. Soc.* **1982**, *104*, 107. (b) Crabtree, R. H. *Acc. Chem. Res.* **1979**, *12*, 331. (c) Shapley, J. R.; Schrock, R. R.; Osborn, J. A. *J. Am. Chem. Soc.* **1969**, *91*, 2816.

[6] Collman, J. P.; Hegedus, L. S.; Norton, J. R.; Finke, R. G. *Principles and Applications of Organotransition Metal Chemistry*, 2nd ed.; University Science Books: Mill Valley, CA, 1987; Chapter 10 and references therein.

[7] Orchin, M. *Acc. Chem. Res.* **1981**, *14*, 259.

[8] (a) Vidal, J. L.; Walker, W. E. *Inorg. Chem.* **1981**, *20*, 249. (b) Whyman, R. *J. Chem. Soc., Dalton Trans.* **1972**, 1375. (c) Whyman, R. *J. Chem. Soc. D* **1969**, 1381.

[9] Csontos, G.; Heil, B.; Marko, L. *Ann. N.Y. Acad. Sci.* **1974**, *239*, 47.

[10] (a) Kruck, T.; Lang, W.; Derner, N. *Z. Naturforsch. B* **1965**, *20*, 705. (b) Kruck, T.; Derner, N.; Lang, W. *Z. Naturforsch., B* **1966**, *21*, 1020. (c) Bennett, M. A.; Patmore, D. J. *Inorg. Chem.* **1971**, *10*, 2387.

[11] (a) Ernst, M. F.; Roddick, D. M. *Inorg. Chem.* **1989**, *28*, 1624. (b) Ernst, M. F.; Roddick, D. M. *Organometallics* **1990**, *9*, 1586. (c) Koola, J. D.; Roddick, D. M. *J. Am. Chem. Soc.* **1991**, *113*, 1450.

[12] Schnabel, R. C.; Roddick, D. M. *Inorg. Chem.*, in press.

0276-7333/93/2312-0704$04.00/0 © 1993 American Chemical Society

Scheme I

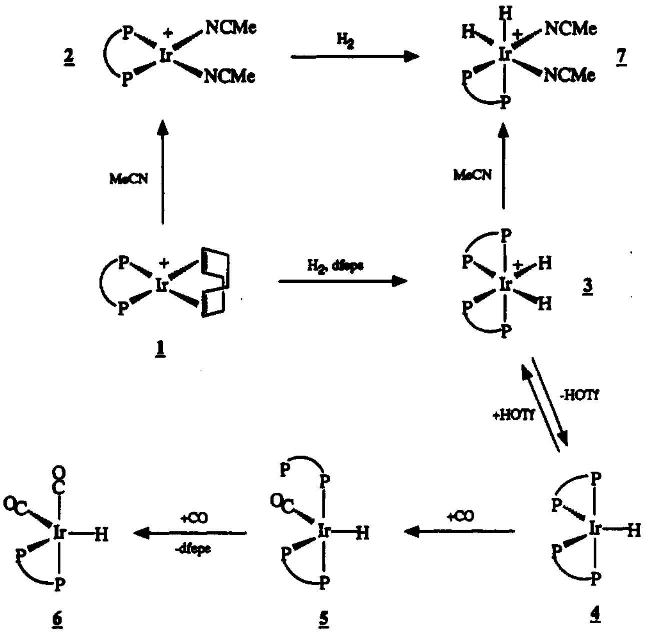

structure of an unusual triflate-bridged trihydrido dimer, $(dfepe)_2Ir_2(H)(\mu\text{-}H)_2(\mu\text{-}O_3SCF_3)$.

Results and Discussion

Synthesis and Reactivity of [(cod)Ir(thf)$_2$]OTf (1). The cationic solvate [(cod)Ir(thf)$_2$]OTf, readily prepared in situ from the reaction of [(cod)Ir(μ-Cl)]$_2$ and AgOTf in thf,[13] provides a convenient entry point to dfepe iridium chemistry (Scheme I). Treatment of a yellow thf solution of [(cod)Ir(thf)$_2$]OTf with dfepe gave a deep red solution from which [(dfepe)Ir(cod)]OTf (1) was obtained as a deep magenta crystalline solid in 80% yield. 1 is soluble in polar organic solvents and is air-stable in the solid state. Although the displacement of coordinated cyclooctadiene from 1 by acetonitrile quantitatively affords [(dfepe)Ir(MeCN)$_2$]OTf (2), treatment of 1 with excess dfepe did not generate [(dfepe)$_2$Ir]OTf. Hydrogenation of 1 in the presence of dfepe at ambient temperature did, however, yield the cationic Ir(I) dihydride *cis*-[(dfepe)$_2$IrH$_2$]OTf (3). The cationic complex 3 is completely insoluble in benzene and ether and is only sparingly soluble in dichloromethane. The cis geometry of 3 was confirmed by its ^{31}P NMR spectrum, which exhibits two broad multiplets at 52.1 and 67.0 ppm. A complex hydride multiplet is observed in the ^1H NMR at δ −13.06, which is similar to that reported for the neutral isoelectronic ruthenium complex *cis*-(dfepe)$_2$RuH$_2$.[11c] 3 is quite stable and may be stored for weeks in dry air without significant decomposition. Deprotonation of 3 readily occurs with mild bases such as diethyl ether or acetone to afford the neutral hydride (dfepe)$_2$IrH (4). 4 is highly fluxional on the NMR time scale at 20 °C, exhibiting a single ^{31}P NMR resonance at 60.7 ppm and a simple pentet at δ −13.40 ($^2J_{PH}$ = 11 Hz) in the ^1H NMR for the hydride ligand. No spectral changes were observed down to −80 °C. The extreme acidity of 3 is apparent in reverse protonation experiments: In the presence of excess $HBF_4 \cdot Et_2O$ no spectral changes are observed in dichloromethane for the hydride resonance of 4, indicating that the equilibrium between [(dfepe)$_2$IrH$_2$]$^+$BF$_4^-$ and 4 under these conditions strongly favors the neutral hydride. *cis*-[(dfepe)$_2$IrH$_2$]OTf is, however, re-formed from (dfepe)$_2$IrH upon treatment with 2 equiv of the stronger acid CF_3SO_3H. These observations may be contrasted with the significantly lower acidities noted for [(dppe)$_2$Ir(R)H]$^+$ and even the dication [(dppe)$_2$Ir(CO)H]$^{2+}$.[14,15]

Table I. Summary of Crystallographic Data for (dfepe)$_2$IrH (4) and (dfepe)$_2$Ir$_2$(H)(μ-H)$_2$(μ-O$_3$SCF$_3$) (9)

	$C_{20}H_9F_{40}IrP_4$	$C_{21}H_{11}F_{43}Ir_2O_3P_4S$
crystal size (mm)	0.30 × 0.40 × 0.58	0.39 × 0.40 × 0.42
cryst system	orthorhombic	monoclinic
space group	$P2_12_12_1$	$P2_1/n$
temp (°C)	−100	−100
a (Å)	11.706(4)	10.915(3)
b (Å)	16.449(5)	19.967(4)
c (Å)	18.497(5)	19.898(5)
β (deg)		102.58(2)
V (Å^3)	3572.5(5)	4232(4)
Z	4	4
ρ_{calc} (g/cm^3)	2.464	2.619
wavelength (Å)	0.710 73	0.710 73
mol wt	1325.3	1668.6
μ (mm^{-1}	4.12	6.67
T_{max}/T_{min}		0.0201/0.0064
2θ range (deg)	4.0–50.0	4.0–45.0
scan type	$2\theta/\theta$	$2\theta/\theta$
scan range	2.0	2.0
no. of rflns measd	4619	6120
no. of unique rflns	4591	5567
no. of rflns with $F > 4\sigma(F)$	3471	3808
R_F (%)	6.45	6.25
R_{wF} (%)	6.65	8.43
goodness of fit	1.22	1.15

In order to differentiate between possible square-pyramidal and dynamic trigonal-bipyramidal ground-state geometries, the solid-state geometry of 4 has been determined by X-ray diffraction. A summary of data collection parameters, atomic coordinates, and metrical parameters are tabulated in Tables I–III. Although the hydride ligand was not found, its approximate location may be inferred from the orientation of the M–P bonds about the iridium center as being in the void space between P(1) and P(4) and roughly in the plane defined by Ir, P(2), and P(3). Assigning an approximate trigonal-bipyramidal geometry is problematic. For prior (dppe)$_2$IrX structures, both axial and equatorial coordination of the unique ligand X has been observed,[16,17] with σ-donor X ligands (X = H, Me) preferring the axial site.[16] A comparison of structural parameters for 4 with (dppe)$_2$IrMe and (dppe)$_2$IrH metrical data is presented in Table IV. P–Ir–P angles for the dppe structures are quite similar and approximate a trigonal-bipyramidal geometry with distortions imposed by the chelating ligands. P_{eq}–Ir–P_{eq} angles for 4, however, deviate significantly from analogous values for (dppe)$_2$IrMe and (dppe)$_2$IrH and are in less accord with an axial TBP geometry. Indeed, the orientation of 4 presented in Figure 1 is more suggestive of equatorial coordination.[18] Any

---

[13] Burk, M. J.; Arduengo, A. J.; Calabrese, J. C.; Harlow, R. L. *J. Am. Chem. Soc.* **1989**, *111*, 8938.

[14] (a) Lilga, M. A.; Sohn, Y. S.; Ibers, J. A. *Organometallics* **1986**, *5*, 766. (b) Vaska, L.; Catone, D. L. *J. Am. Chem. Soc.* **1966**, *88*, 5324.

[15] Lilga, M. A.; Ibers, J. A. *Inorg. Chem.* **1984**, *23*, 3538.

[16] Axial (dppe)$_2$MX structures: (a) Lilga, M. A.; Sohn, Y. S.; Ibers, J. A. *Organometallics* **1986**, *5*, 766. (b) Teo, B.-K.; Ginsberg, A. P.; Calabrese, J. C. *J. Am. Chem. Soc.* **1976**, *98*, 3027.

[17] Equatorial (dppe)$_2$MX structures: (a) Goldberg, S. Z.; Eisenberg, R. *Inorg. Chem.* **1976**, *15*, 58. (b) Jarvis, J. A. J.; Mais, R. H. B.; Owston, P. G.; Taylor, K. A. *Chem. Commun.* **1966**, 906.

[18] The phosphine chelate disposition in 4 is comparable to that found for *cis*-(dfepe)$_2$RuH$_2$[19] or *cis*-(dppe)$_2$RuH$_2$,[20] which have equatorial hydride ligands and P_{ax}–Ru–P_{ax} angles of 155 and 161°, respectively.

Table II. Atomic Coordinates (×10^4) and Equivalent Isotropic Displacement Coefficients (Å^2 × 10^3) for (dfepe)$_2$IrH (4)

	x	*y*	*z*	*U*(eq)[a]
Ir	9874(1)	9732(1)	642(1)	27(1)
P(1)	9261(5)	8929(3)	1537(3)	41(2)
P(2)	8245(4)	10447(3)	901(3)	34(2)
P(3)	11592(4)	10388(4)	757(3)	34(2)
P(4)	10249(5)	9759(3)	–560(2)	40(1)
C(1)	7839(18)	9194(14)	1858(12)	45(7)
C(2)	7603(24)	10097(22)	1782(15)	77(12)
C(3)	8884(30)	7797(21)	1361(19)	83(9)
C(4)	9952(44)	7181(13)	1232(18)	106(17)
C(5)	10036(17)	8792(10)	2430(9)	33(4)
C(6)	10016(23)	9523(12)	2921(11)	50(7)
C(7)	8299(20)	11576(16)	1065(14)	50(6)
C(8)	7286(23)	1215(18)	1291(16)	57(10)
C(9)	6907(17)	10457(12)	333(11)	38(5)
C(10)	6476(22)	9718(20)	8(13)	64(9)
C(11)	12207(17)	10558(17)	–154(11)	48(7)
C(12)	11771(19)	9934(14)	–687(12)	53(7)
C(13)	11710(18)	11457(13)	1193(12)	40(5)
C(14)	12872(23)	11936(18)	1251(19)	62(11)
C(15)	12838(19)	9892(15)	1234(13)	51(6)
C(16)	13193(27)	9011(20)	1013(15)	67(11)
C(17)	9643(16)	10617(12)	–1155(10)	36(4)
C(18)	10113(18)	10807(12)	–1892(11)	43(6)
C(19)	10593(15)	8796(15)	–1089(10)	100
C(20)	9473(12)	8383(9)	–1318(9)	100
F(1)	8280(14)	7802(11)	734(10)	83(5)
F(2)	8224(15)	7503(11)	1880(11)	83(5)
F(3)	10559(18)	7420(10)	682(11)	99(8)
F(4)	10528(29)	7141(12)	1805(11)	147(14)
F(5)	9410(24)	6471(9)	1063(10)	117(10)
F(6)	9606(12)	8190(9)	2851(8)	63(4)
F(7)	11178(11)	8627(8)	2288(7)	52(3)
F(8)	10340(14)	10184(7)	2579(7)	65(5)
F(9)	10765(13)	9383(10)	3476(8)	66(5)
F(10)	9026(11)	9655(11)	3230(7)	64(5)
F(11)	8789(10)	11946(7)	493(7)	45(3)
F(12)	9045(11)	11660(8)	1622(7)	50(3)
F(13)	6751(15)	11801(14)	1849(10)	96(8)
F(14)	7720(18)	12865(12)	1451(12)	100(9)
F(15)	6606(12)	12244(10)	731(10)	73(6)
F(16)	7046(12)	10997(9)	–227(8)	56(3)
F(17)	5989(12)	10748(10)	715(9)	70(4)
F(18)	5522(13)	9810(14)	–337(9)	95(7)
F(19)	7213(14)	9366(10)	–468(10)	80(6)
F(20)	6290(15)	9133(12)	502(10)	90(7)
F(21)	11034(11)	11901(8)	743(7)	52(3)
F(22)	11298(10)	11423(8)	1838(7)	45(3)
F(23)	13476(12)	11889(9)	633(11)	70(6)
F(24)	13460(13)	11703(11)	1777(10)	75(6)
F(25)	12570(14)	12715(10)	1375(12)	84(8)
F(26)	13809(12)	10370(10)	1132(8)	65(4)
F(27)	12652(11)	9907(8)	1954(8)	52(3)
F(28)	12380(15)	8486(11)	1148(10)	82(7)
F(29)	14117(15)	8833(11)	1416(10)	85(7)
F(30)	13442(14)	8972(12)	344(9)	73(7)
F(31)	8464(11)	10491(8)	–1231(7)	57(4)
F(32)	9797(11)	11277(8)	–757(7)	59(3)
F(33)	9854(14)	10215(9)	–2358(6)	68(5)
F(34)	9441(15)	11445(9)	–2155(8)	78(6)
F(35)	11109(12)	10992(8)	–1899(8)	61(5)
F(36)	10913(15)	8946(11)	–1776(10)	84(5)
F(37)	11060(20)	8154(15)	–748(13)	126(8)
F(38)	8970(12)	8092(9)	–716(9)	132(5)
F(39)	9737(12)	7764(9)	–1762(9)	132(5)
F(40)	8751(12)	8894(9)	–1657(9)	132(5)

[a] Equivalent isotropic *U* defined as one-third of the trace of the orthogonalized $\mathbf{U}_{ij}$ tensor.

attempt to reconcile the geometry of 4 with an idealized 5-coordinate geometry must be viewed with some caution.

Table III. Selected Distances (Å) and Angles (deg) for (dfepe)$_2$IrH (4)

	Bond Distances		
Ir–P(1)	2.242(6)	Ir–P(2)	2.298(5)
Ir–P(3)	2.298(5)	Ir–P(4)	2.269(5)
P(1)–C(1)	1.82(2)	P(1)–C(3)	1.95(4)
P(1)–C(5)	1.90(2)	P(2)–C(2)	1.89(3)
P(2)–C(7)	1.89(3)	P(2)–C(9)	1.89(2)
P(3)–C(11)	1.86(2)	P(3)–C(13)	1.95(2)
P(3)–C(15)	1.89(2)	P(4)–C(12)	1.82(2)
P(4)–C(17)	1.93(2)	P(4)–C(19)	1.91(2)
	Bond Angles		
P(1)–Ir–P(2)	83.2(2)	P(1)–Ir–P(3)	119.4(2)
P(1)–Ir–P(4)	110.9(2)	P(2)–Ir–P(3)	117.9(2)
P(2)–Ir–P(4)	110.9(2)	P(3)–Ir–P(4)	84.9(2)

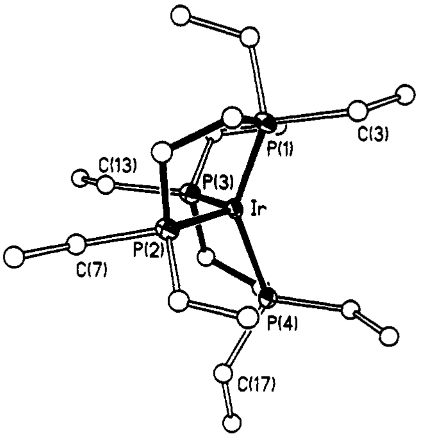

Figure 1. ORTEP view of (dfepe)$_2$IrH (4) with atom-labeling scheme.

The average Ir–P bond distance for 4 (2.277 Å) is intermediate between the average values for (dppe)$_2$IrMe (2.281 Å) and (dppe)$_2$IrH (2.268 Å). The absence of any significant M–P bond shortening for the dfepe ligand relative to dppe contrasts with monochelate studies (vide infra)[11,12] and may reflect either a diminished M–P π back-bonding distributed between the four phosphorus centers in 4 or simply increased steric congestion about the metal center.

(dfepe)$_2$IrH has significant thermal stability in solution and in the solid state (mp 135–138 °C). No loss of dfepe is observed in acetonitrile after warming to 90 °C for 14 h. Treatment of 4, however, with 1 atm of carbon monoxide in acetone at ambient temperature results in the displacement of one dfepe ligand. After 15 min, a quartet hydride resonance at –13.40 ($^2J_{PH}$ = 21 Hz) is observed by ^{1}H NMR together with new ^{31}P NMR multiplets at δ 59.2, 42.7, and 8.5. A single transient carbonyl band at 2116 cm^{-1} confirms the identity of this intermediate as the initial chelate displacement adduct (dfepe)(η^1-dfepe)Ir(CO)H (5). After 2 h the substitution of one dfepe by two CO ligands is complete to give the dicarbonyl hydride (dfepe)Ir(CO)$_2$H (6) (ν(CO) = 2051, 2009 cm^{-1}). The triplet hydride resonance observed for 6 (δ –10.20, $^2J_{PH}$ = 57 Hz) compares closely to that reported for (dppe)Ir(CO)$_2$H[21] and is consistent with a fluxional 5-coordinate geometry.

In contrast to the neutral hydride 4, displacement of one dfepe ligand from [(dfepe)IrH$_2$]OTf in acetonitrile at 20 °C readily occurs to form the bis(solvate) [(dfepe)Ir(MeCN)$_2$(H)$_2$]OTf (7) (ν(MeCN) = 2329, 2301 cm^{-1}). Inequivalent phosphorus, hydride, and acetonitrile methyl group resonances observed by NMR are indicative of a cis

---

(19) Koola, J. D.; Roddick, D. M. Unpublished results.

(20) Pertici, P.; Vitulli, G.; Porzio, W.; Zocchi, M. *Inorg. Chim. Acta* **1979**, *37*, L521.

(21) Fisher, B. J.; Eisenberg, R. *Organometallics* **1983**, *2*, 764.

Table IV. Comparison of Structural Parameters for 4 with Those for $(dppe)_2IrX$ (X = H, Me) Complexes

complex[a]	M–P_{ax} (Å)	M–P_{eq} (Å)	X–M–P_{ax} (deg)	X–M–P_{eq} (deg)	P_{eq}–M–P_{eq} (deg)	P_{ax}–M–P_{eq} (deg)
$(dppe)_2IrMe$[b]	2.283(2)	2.264(2)	164.7(2)	88.7(3)	145.7(1)	106.2(1)
		2.274(2)		84.1(2)	123.5(1)	100.2(1)
		2.304(2)		83.3(2)	88.0(1)	84.8(1)
$(dppe)_2IrH$[c]	2.278(2)	2.245(2)			141.9(1)	107.0(1)
		2.271(2)			125.1(1)	106.1(1)
		2.279(2)			87.6(1)	84.0(1)
$(dfepe)_2IrH$	2.298(5)	2.298(5)			143.1(2)	119.4(2)
		2.269(5)			110.9(2)	117.9(2)
		2.242(6)			83.2(2)	84.9(2)
$(dppe)_2Ir(CO)^+$[d]	2.37(2)	2.37(2)	143(2)	109(2)	176(1)	108(1)
		2.37(2)		91(1)	97(1)	97(1)
		2.37(2)		91(1)	83(1)	83(1)
$(dppe)_2Ir(CNMe)^+$[e]	2.324(3)	2.345(3)	132.7(2)	106.9(3)	176.2(1)	120.4(1)
		2.338(3)		89.3(3)	97.6(1)	98.3(1)
		2.306(3)		87.2(3)	84.6(1)	83.2(1)

[a] Axial and equatorial labels are assigned assuming that the unique ligand and the phosphorus ligand with the largest angle with respect to it are axial. [b] Reference 16a. [c] Reference 16b. [d] Reference 17b. [e] Reference 17a.

octahedral stereochemistry for 7 as shown in Scheme I. In accordance with $^2J_{PH}$ values and empirical chemical shift trends noted elsewhere,[22] the hydride resonances at δ −7.31 and −19.73 are readily assigned to hydride ligands trans to dfepe and MeCN, respectively. Complex 7 may also be prepared independently by the hydrogenolysis of $[(dfepe)Ir(MeCN)_2]OTf$.

Reaction of $[(dfepe)Ir(cod)]OTf$ (1) with H_2. Ir(V) and Ir(III) polyhydrido products $(R_3P)_2IrH_5$, $(R_3P)_4Ir_2H_5^+$, and $(R_3P)_6Ir_3H_7^{2+}$ have been isolated from the hydrogenolysis of $[(R_3P)_2Ir(cod)]^+A^-$ (A^- = BF_4^-, PF_6^-) complexes in the absence of donor ligands or solvents.[23,24] For [(dfepe)Ir(cod)](OTf), exposure of a red CH_2Cl_2 solution to 1 atm of H_2 at ambient temperature results in rapid bleaching and precipitation of the sparingly soluble pale yellow crystalline product 8. Infrared and ^1H and ^{31}P NMR data are in accord with the neutral dimeric triflate structure $[(dfepe)Ir(H)(\mu\text{-}H)(OTf)]_2$ having an 18-electron octahedral iridium environment (Scheme II). ^1H NMR data for the $Ir_2(H)_2(\mu\text{-}H)_2$ core exhibit bridging and terminal hydride multiplets at δ −6.43 (br d, $^2J_{PH}$(trans) = 153 Hz) and −29.83 (t, $^2J_{PH}$(cis) = 6 Hz), respectively, which are integrated as two protons apiece versus the dfepe backbone resonances. Efforts to obtain ^{31}P NMR data for 8 were hampered by poor solubility in CH_2Cl_2 and its reactivity with even weakly basic solvents (see below); however, 8 is moderately soluble and sufficiently stable in *o*-difluorobenzene for characterization. The observance of only one ^{31}P resonance in this solvent is indicative of a symmetrical ligand environment with equatorial dfepe coordination as drawn above. Unidentate triflate coordination is indicated by $\nu(SO_3)$ IR bands at 1324 and 1017 cm^{-1}, which are shifted in the expected manner from free ion triflate stretches (~1280, ~1040 cm^{-1}).[25,26] For comparison, the lower energy $\nu(SO_3)$ stretch for uncoordinated triflate in complexes 1, 2, and 7 is found between 1030 and 1034 cm^{-1}.

The tetrahydride dimer 8 may be formally viewed as a doubly protonated derivative of the dihydride dimer $[(dfepe)Ir(\mu\text{-}H)]_2$. Indeed, dissolving 8 in acetone results in the quantitative loss of 1 equiv of CF_3SO_3H and formation of the asymmetrical trihydride $(dfepe)_2Ir_2(\mu\text{-}H)_2(H)(\mu\text{-}O_3SCF_3)$ (9). Although bridging (δ −5.53) and terminal (δ −27.65) hydride resonances for 9 are shifted only slightly from values for 8, the integrated Ir(μ-H)/Ir(H) ratio is 2:1. The asymmetry suggested by ^1H NMR data is consistent with ^{31}P NMR data and has been confirmed by the solid-state structure of 9 (see below). Attempts to further deprotonate 9 have not been successful. Treatment of 9 with excess diethylamine in dichloromethane yields the previously prepared Et_2NH adduct $(dfepe)Ir(Et_2NH)Cl$,[12] possibly derived from attack by a reactive $[(dfepe)Ir(\mu\text{-}H)]_2$ intermediate on dichloromethane. Although displacement of the triflate bridge and formation of the base adduct 10 might be expected as an alternative reaction pathway, monitoring of this reaction by ^1H NMR revealed no resonances other than those of 9 and $(dfepe)Ir(Et_2NH)Cl$. No products from the addition of basic reagents to 9 in hydrocarbon or aromatic solvents have been isolated.

Scheme II

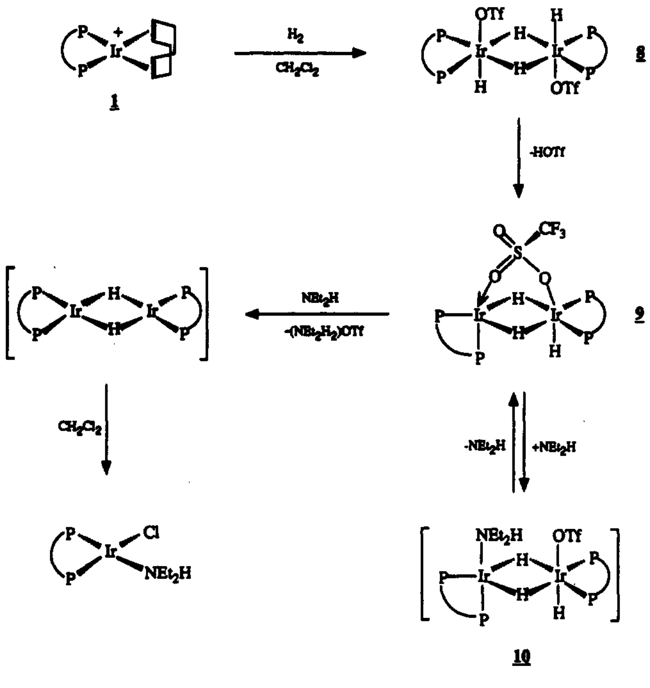

Crystal Structure of $(dfepe)_2Ir_2(\mu\text{-}H)_2(H)(O_3SCF_3)$

---

(22) Crabtree, R. H.; Demou, P. C.; Eden, D.; Mihelcic, J. M.; Parnell, C. A.; Quirk, J. M.; Morris, G. E. *J. Am. Chem. Soc.* **1982**, *104*, 6994.

(23) (a) Crabtree, R. H.; Felkin, H.; Morris, G. E. *J. Organomet. Chem.* **1977**, *141*, 205. (b) Crabtree, R. H.; Felkin, H.; Morris, G. E.; King, T. J.; Richards, J. A. *J. Organomet. Chem.* **1976**, *113*, C7.

(24) Wang, H. H.; Pignolet, L. H. *Inorg. Chem.* **1980**, *19*, 1470.

(25) (a) Batchelor, R. J.; Ruddick, J. N. R.; Sams, J. R.; Aubke, F. *Inorg. Chem.* **1977**, *16*, 1414. (b) Bürger, H.; Burczyk, K.; Blaschette, A. *Monatsh. Chem.* **1970**, *101*, 102.

(26) Blake, D. M. *J. Chem. Soc., Chem. Commun.* **1974**, 815.

Table V. Atomic Coordinates (×10⁴) and Equivalent Isotropic Displacement Coefficients (Å² × 10³) for $(dfepe)_2Ir_2(H)(\mu\text{-}H)_2(\mu\text{-}O_3SCF_3)$ (9)

	x	*y*	*z*	*U*(eq)[a]		*x*	*y*	*z*	*U*(eq)[a]
Ir(1)	611(1)	7867(1)	1941(1)	41(1)	F(7)	4165(14)	6650(8)	1871(8)	79(4)
Ir(2)	−848(1)	6767(1)	2136(1)	42(1)	F(8)	3061(18)	6289(10)	658(9)	102(5)
P(1)	2471(5)	7458(3)	2205(3)	44(2)	F(9)	1328(15)	6778(8)	680(8)	79(4)
P(2)	1565(5)	8793(3)	1814(3)	49(2)	F(10)	2990(16)	7348(9)	694(9)	94(5)
P(3)	−1735(6)	5837(3)	1601(3)	57(2)	F(11)	12(15)	8747(8)	1804(8)	83(4)
P(4)	−1555(5)	6374(3)	3043(3)	52(2)	F(12)	1987(14)	10066(7)	2218(7)	73(4)
S(1)	−2405(5)	8177(3)	1698(3)	53(2)	F(13)	−65(15)	9130(8)	2953(8)	79(4)
O(1)	−2499(13)	7463(7)	1776(7)	49(5)	F(14)	598(15)	10137(8)	3164(9)	87(5)
O(2)	−1150(14)	8373(7)	1670(8)	57(6)	F(15)	1835(17)	9293(9)	3340(9)	96(5)
O(3)	−3017(18)	8577(10)	2113(8)	82(8(	F(16)	1764(15)	9787(8)	897(8)	79(4)
C(1)	3695(19)	8058(10)	2122(11)	44(7)	F(17)	2548(15)	8806(8)	715(8)	84(4)
C(2)	3232(20)	8780(10)	2187(11)	51(8)	F(18)	575(16)	9212(8)	−272(9)	87(5)
C(3)	−2294(38)	5268(16)	2227(15)	107(16)	F(19)	263(17)	8277(9)	258(9)	97(5)
C(4)	−2596(25)	5673(15)	2780(12)	74(11)	F(20)	−596(16)	9210(9)	497(9)	92(5)
C(5)	3026(22)	7096(12)	3078(12)	54(6)	F(21)	−117(17)	5605(9)	790(10)	98(5)
C(6)	2992(26)	2599(14)	3701(14)	69(7)	F(22)	381(16)	5171(9)	1818(9)	89(5)
C(7)	2943(20)	6759(11)	1684(11)	48(5)	F(23)	−1256(26)	4218(14)	1493(14)	158(9)
C(8)	2560(28)	6804(15)	932(15)	77(8)	F(24)	−1771(27)	4570(14)	427(14)	161(10)
C(9)	1118(25)	9609(13)	2187(13)	65(7)	F(25)	17(20)	4279(11)	849(11)	116(6)
C(10)	858(23)	9541(12)	2921(13)	60(6)	F(26)	−3773(18)	5241(10)	779(10)	110(6)
C(11)	1550(24)	9132(13)	917(12)	62(6)	F(27)	−3963(16)	6267(9)	1184(9)	96(5)
C(12)	466(26)	8951(15)	342(14)	75(7)	F(28)	−2503(24)	5785(13)	−118(13)	144(8)
C(13)	−582(25)	5260(14)	1273(14)	70(7)	F(29)	−2521(24)	6667(14)	258(13)	144(8)
C(14)	−948(40)	4561(21)	1027(23)	115(12)	F(30)	−4299(23)	6230(12)	−159(13)	142(8)
C(15)	−3166(27)	5878(14)	928(15)	74(7)	F(31)	−3139(14)	6567(8)	3890(8)	79(4)
C(16)	−3145(32)	6153(18)	258(17)	92(9)	F(32)	−3490(14)	7150(8)	2928(8)	77(4)
C(17)	−2547(23)	6940(12)	3496(12)	60(6)	F(33)	−2899(18)	7886(10)	4032(10)	101(5)
C(18)	−1995(24)	7563(14)	3871(13)	64(6)	F(34)	−1203(17)	7380(9)	4426(10)	99(5)
C(19)	−401(21)	6030(12)	3823(11)	54(6)	F(35)	−1446(17)	7923(9)	3475(9)	95(5)
C(20)	246(33)	5491(18)	3805(19)	97(10)	F(36)	483(15)	6525(8)	4029(8)	82(4)
C(21)	−3247(20)	8328(15)	843(13)	63(10)	F(37)	−970(17)	5973(9)	4441(9)	100(5)
F(1)	2350(12)	6546(7)	3161(7)	64(3)	F(38)	829(17)	5457(9)	3299(9)	98(5)
F(2)	4229(14)	6874(7)	3187(7)	71(4)	F(39)	1056(24)	5328(13)	4426(13)	145(8)
F(3)	1826(14)	7750(8)	3703(8)	78(4)	F(40)	−402(24)	4940(13)	3739(13)	143(8)
F(4)	3656(16)	8111(8)	3659(9)	88(5)	F(41)	−2814(18)	8035(9)	386(7)	93(7)
F(5)	3478(16)	7279(8)	4295(9)	88(5)	F(42)	−3267(15)	8971(10)	686(8)	97(8)
F(6)	2405(13)	6152(7)	1879(7)	68(4)	F(43)	−4414(16)	8132(11)	760(10)	112(9)

[a] Equivalent isotropic *U* defined as one-third of the trace of the orthogonalized U_{ij} tensor.

Table VI. Selected Distances (Å) and Angles (deg) for $(dfepe)_2Ir_2(\mu\text{-}H)_2(H)(O_3SCF_3)$ (9)

	Bond Distances		
Ir(1)–Ir(2)	2.789(1)	Ir(1)–P(1)	2.145(5)
Ir(1)–P(2)	2.164(6)	Ir(1)–O(2)	2.135(15)
Ir(2)–P(3)	2.251(6)	Ir(2)–P(4)	2.251(6)
Ir(2)–O(1)	2.266(14)	S(1)–O(1)	1.44(1)
S(1)–O(2)	1.44(2)	S(1)–O(3)	1.42(2)
S(1)–C(21)	1.78(2)		
	Bond Angles		
Ir(2)–Ir(1)–P(1)	101.8(2)	Ir(2)–Ir(1)–P(2)	173.2(2)
P(1)–Ir(1)–P(2)	84.3(2)	Ir(2)–Ir(1)–O(2)	84.2(4)
P(1)–Ir(1)–O(2)	173.9(4)	P(2)–Ir(1)–O(2)	89.6(4)
Ir(1)–Ir(2)–P(3)	141.6(2)	Ir(1)–Ir(2)–P(4)	133.8(2)
p(3)–Ir(2)–P(4)	84.5(2)	Ir(1)–Ir(2)–O(1)	84.9(4)
P(3)–Ir(2)–O(1)	97.3(4)	P(4)–Ir(2)–O(1)	94.5(4)
Ir(1)–O(2)–S(1)	132.3(10)	Ir(2)–O(1)–S(1)	124.8(8)
O(1)–S(1)–O(2)	111.5(9)	O(1)–S(1)–O(3)	116(1)
O(2)–S(1)–O(3)	116(1)	O(1)–S(1)–C(21)	104(1)
O(2)–S(1)–C(21)	103(1)	O(3)–S(1)–C(21)	105(1)

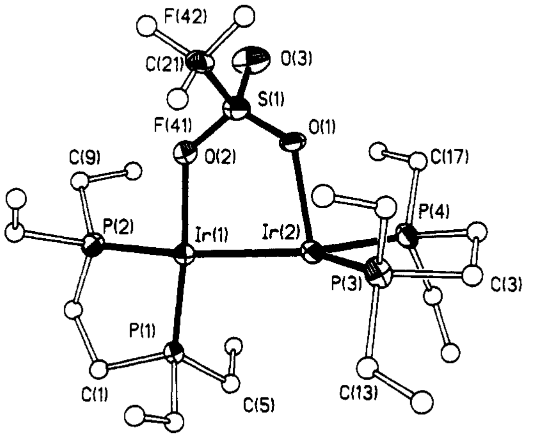

Figure 2. ORTEP view of $(dfepe)_2Ir_2(H)(\mu\text{-}H)_2(\mu\text{-}O_3SCF_3)$ (9) with atom-labeling scheme.

(9). The dimeric formulation of hydride complexes 8 and 9 has been verified by a structural analysis of 9. Selected metrical parameters are given in Table VI. As shown in Figure 2, the coordination environment about each iridium center is distinct. Although the positions of the hydride ligands could not be reliably determined, the observed Ir(1)–Ir(2) distance of 2.789(1) Å is significantly longer than Ir–Ir distances reported for the triply bridged dimers $(Ph_3P)_4Ir_2H_5^+$ (2.518 Å)[23] and $(dppp)_2Ir_2H_5^+$ (2.514 Å)[24] and comparable to the average value for the doubly hydride bridged trimer $(dppp)_3Ir_3H_7^+$ of 2.772 Å.[24] A consideration of void spaces about the Ir(2) center indicates that the unique terminal hydride must be located trans to the O(1) triflate oxygen. Hydride positions are also manifested in the variation of observed Ir–P bond lengths. The Ir(2)–P(3) and Ir(2)–P(4) bonds, which are trans to the bridging hydride ligands, are approximately 0.1 Å longer than Ir(1)–P(1) (2.144(5) Å) and Ir(1)–P(2) (2.162(5) Å). The latter bond lengths are comparable to values for dfepe ligation trans to weaker chloride and amine donor ligands in $(dfepe)Ir(NEt_2H)Cl$ of 2.151(2) and 2.165(2) Å, respectively.[12]

Complex 9 represents one of the few structurally characterized examples of bidentate bridging triflate coordination to a transition metal.[27] From the standpoint of formal valence electron counting, the molecule may be best described as a coordinatively saturated mixed-valence Ir(I)–Ir(III) dimer with an unsymmetrical (localized) triflate bridge. Metrical evidence, however, does not support this bonding picture. Any argument regarding the relative Ir–O bond lengths expected for localized triflate bonding is complicated by trans ligand effects, since the difference between Ir(2)–O(1) (2.27(1) Å) and Ir(1)–O(2) (2.14(1) Å) is comparable to the variation in Ir–P bond lengths between the Ir(1) and Ir(2) centers. In addition, the chelate S–O bond lengths S(1)–O(1) and S(1)–O(2) are effectively identical and do not indicate the presence of a localized double bond between S(1) and O(2). Symmetrical μ-OTs binding to an asymmetric Rh_2^{4+} core has been observed previously.[28]

Summary. With the exception of $(dfepe)_2Ir^+$, the synthesis of $(dfepe)(L)_2Ir^+$ and $(dfepe)(L)_2Ir(H)_2^+$ complexes is relatively straightforward and follows established methodologies for donor phosphine systems. The extremely high apparent acidity of $(dfepe)_2Ir(H)_2^+$ (**3**) clearly reflects the electron-poor nature of the formally Ir(III) center in **3** and is in accord with the high acidity of the binuclear Ir(III) polyhydride complex **8** as well as other $(dfepe)M(H)_2^+$ systems.[29] The high thermal and air stability of $(dfepe)_2IrH$ (**4**) is exceptional when compared to those of known $(R_3P)_4IrH$ complexes. The displacement of one dfepe ligand from **4** by CO to form $(dfepe)Ir(CO)_2H$ parallels chemistry reported for *cis*-$(dfepe)_2Ru(H)_2$ and is consistent with the relatively long M–P bond lengths found for $(dfepe)_2M$ structures. This lability may be attributed to either sterically induced chelate loss or acceptor competition for electron density as found in labile polycarbonyl systems.

A clear comparison of [(dfepe)Ir(cod)]OTf (**1**) hydrogenolysis chemistry with known $[(R_3P)_2Ir(cod)]^+$ chemistry is complicated by counterion effects. For donor phosphine systems, cationic Ir(III) polyhydride dimers and trimers are obtained using BF_4^- or PF_6^- counterions. The triflate ion $CF_3SO_3^-$ is generally considered to be a weakly coordinating counteranion;[30] however, in the electron-poor dfepe systems examined, OTf^- coordination is preferred. Facile loss of HOTf from **8** to give the mixed Ir(I)–Ir(III) dimer **9** has been demonstrated, although further deprotonation to give the Ir(I)–Ir(I) dimer $[(dfepe)Ir(\mu\text{-}H)]_2$ has thus far proved unsuccessful due to the highly reactive nature of this parent compound. We are presently examining the hydride transfer reactivity properties of (dfepe)Ir systems and examining alternative routes to simple Ir(I) and Ir(III) (fluoroalkyl)phosphine hydrides of the general form $[(dfepe)Ir(H)_x]_n$ (x = 1–3, n = 1, 2).

Experimental Section

General Procedures. All manipulations were conducted under an atmosphere of nitrogen by using Schlenk, high-vacuum-line, and/or glovebox techniques. Dry, oxygen-free solvents were vacuum-distilled prior to use. Elemental analyses were performed by Desert Analytics. Infrared spectra were recorded on a Mattson Cygnus 100 or Perkin-Elmer 1600 FTIR instrument as Nujol mulls, unless otherwise noted. NMR spectra were obtained with a JEOL JMN-FX270 or GSX-400 instrument. ^{19}F spectra were referenced to CF_3CO_2Et as an internal standard (−75.32 ppm vs $CFCl_3$ with downfield chemical shifts taken to be positive). ^{31}P spectra were referenced to an 85% H_3PO_4 external standard. $[(cod)Ir(\mu\text{-}Cl)]_2$ was prepared by following literature procedures,[31] with the exception that 2-propanol instead of ethanol was used as solvent; yields obtained using this modification were generally in excess of 90%. $(C_2F_5)_2PCH_2CH_2P(C_2F_5)_2$ (dfepe) was prepared as described previously.[11a]

$[(dfepe)Ir(C_8H_{12})]O_3SCF_3$ (1). A mixture of 0.570 g (0.848 mmol) of $[(cod)Ir(\mu\text{-}Cl)]_2$ and 0.470 g (1.829 mmol) of silver triflate was taken up in 25 mL of THF and stirred in the dark for 2 h. The resulting yellow solution was filtered, and 1.104 g (1.951 mmol) of dfepe was added dropwise to the filtrate via syringe. The solution turned dark red upon addition, and within a few minutes a deep red crystaline solid began to precipitate. After the mixture was stirred for an additional 1 h, the solvent was reduced to 2 mL, and 5 mL of Et_2O was slowly added to precipitate 2.051 g (80% of **1**. Anal. Calcd for $C_{19}H_{16}F_{23}IrO_3P_2S$: C, 22.47; H, 1.59. Found: C, 22.45; H, 1.40. IR (cm^{-1}): 1298 vs, 1222 vs, 1131, vs, 1032 s, 960 s, 863 m, 805 m, 751 s, 637 s. ^1H NMR (acetone-d_6, 400 MHz, 20 °C): δ 6.58 (br s, 4H; $(CH_2CH{=}CHCH_2)_2$), 3.15 (m, 4H; PCH_2), 2.91 (m, 4H; $(CH_2\text{-}CH{=}CHCH_2)_2$), 2.43 (m, 4H; $(CH_2CH{=}CHCH_2)_2$). ^{31}P NMR (acetone-d_6, 161.9 MHz, 20 °C): δ 78.30 (m). ^{19}F NMR ($CDCl_3$, 376.05 MHz, 20 °C): δ −78.75 (s; O_3SCF_3), −79.04 (s; PCF_2CF_3), −107.18 (dd, $^2J_{FF}$ = 320 Hz, $^2J_{PF}$ = 53 Hz; PCF_2CF_3), −110.25 (dd, $^2J_{FF}$ = 320 Hz, $^2J_{PF}$ = 77 Hz; PCF_2CF_3).

$[(dfepe)Ir(CH_3CN)_2]O_3SCF_3$ (2). A solution of 0.350 g of **1** in 20 mL of acetonitrile was stirred at room temperature for 30 min, during which time the color faded from red to yellow. After removal of MeCN, precipitation from a CH_2Cl_2/Et_2O mixture gave 0.335 g (95%) of bright yellow **2**. Anal. Calcd for $C_{17}H_{10}F_{23}IrO_3P_2S$: C, 18.19; H, 1.01. Found: C, 18.06; H, 0.93. IR (cm^{-1}): 1312 vs, 1276 s, 1223 vs, 1134 vs, 1034 vs, 974 vs, 811 m, 751 s, 720 m, 640 s, 592 w, 574 w, 557 m, 518 s, 474 s. ^1H NMR (acetone-d_6, 400 MHz, 20 °C): δ 2.82 (br, s, 6H; CH_3CN), 2.72 (m, 4H; PCH_2). ^{31}P NMR (acetone-d_6, 161.9 MHz, 20 °C): δ 72.8 (m). ^{19}F NMR (acetone-d_6, 376.05 MHz, 20 °C): δ −78.45 (s; O_3SCF_3), −78.81 (s; PCF_2CF_3), −112.22 (dd, $^2J_{FF}$ = 320 Hz, $^2J_{PF}$ = 57 Hz; PCF_2CF_3), −114.15 (dd, $^2J_{FF}$ = 320 Hz, $^2J_{PF}$ = 57 Hz; PCF_2CF_3).

$[(dfepe)_2IrH_2]O_3SCF_3$ (3). A 0.100-g (0.075-mmol) amount of **1** and 13.5 μL (0.150 mmol) of HO_3SCF_3 were combined in 20 mL of CH_2Cl_2 and stirred at room temperature for 1 h. The solvent was removed, and the residue was triturated with petroleum ether. Filtering and washing the resulting off-white precipitate several times with petroleum ether and drying under vacuum yielded 0.890 g (89%) of analytically pure **3**. Anal. Calcd for $C_{21}H_{10}F_{43}IrO_3P_4S$: C, 17.08; H, 0.68. Found: C, 16.79; H, 0.74. IR (cm^{-1}): 1300 vs, 1207 vs, 1132 s, 1093 s, 954 s, 876 w, 817 m, 749 m, 721 w. ^1H NMR (acetone-d_6, 269.7 MHz, 20 °C): δ 2.25 (m, 4H, PCH_2), −13.06 (dm, $^2J_{PH}$(trans) ≈ 130 Hz, 2H; IrH). ^{31}P NMR (acetone-d_6, 161.9 MHz, 20 °C): δ 67.0 (m), 52.1 (m). ^{19}F NMR (acetone-d_6, 376.05 MHz, 20 °C): δ −76.27, −76.94, −77.59 (s; PCF_2CF_3), −97.2 to −108.3 (overlapping ABX multiplets; PCF_2CF_3).

$(dfepe)_2IrH$ (4). A mixture of 0.505 g (0.497 mmol) of **1** and 0.335 g (0.592 mmol) of dfepe was taken up in 20 mL of CH_2Cl_2 and stirred at room temperature under 1 atm of H_2. During this time the solution changed from dark red to light yellow. After 2 h the solution was cooled to −78 °C, the H_2 was removed, and 0.073 mL (1.143 mmol) of Me_3N was added. After the mixture was stirred at 0 °C for 30 min, the solvent was removed and the

---

[27] Reported μ_2-OTf structures: (a) O'Connor, J. M.; Uhrhammer, R.; Rheingold, A. L.; Staley, D. L. *J. Am. Chem. Soc.* **1989**, *111*, 7633. (b) Richmond, T. G.; Kelson, E. P.; Arif, A. M. *J. Am. Chem. Soc.* **1988**, *110*, 2334. (c) Ferrara, J. D.; Tessier-Youngs, C.; Youngs, W. J. *Inorg. Chem.* **1988**, *27*, 2201. (d) Balch, A. L.; Olmstead, M. M.; Rowley, S. P. *Inorg. Chem.* **1988**, *27*, 2275. (e) Dedert, P. L.; Sorrell, T.; Marks, T. J.; Ibers, J. A. *Inorg. Chem.* **1982**, *21*, 3506.

[28] Clegg, W.; Akhter, L.; Garner, C. D. *J. Chem. Soc., Chem. Commun.* **1984**, 101.

[29] Keady, M. S.; Koola, J. D.; Ontko, A. C.; Merwin, R. K.; Roddick, D. M. *Organometallics* **1992**, *11*, 3417.

[30] Lawrance, G. A. *Chem. Rev.* **1986**, *86*, 17.

[31] Herde, J. L.; Lambert, J. C.; Senoff, C. V. *Inorg. Synth.* **1974**, *15*, 18.

residue was repeatedly extracted with $\mathrm{Et_2O}$. Concentration of the filtrate to 2 mL and cooling to −78 °C afforded after cold filtration and drying 0.375 g (54%) of off-white **4** (mp 135–138 °C). Anal. Calcd for $\mathrm{C_{20}H_9F_{40}Ir}$: C, 18.11; H, 0.67. Found: C, 18.05; H, 0.55. IR (cm^{-1}): 1377 w, 1294 s, 1225 s, 1134 s, 1098 s, 964 s, 876 w, 817 m, 749 m. ^{1}H NMR (acetone-d_6, 269.7 MHz, 20 °C): δ 2.67 (m, 8H; PCH_2), −13.40 (p, $^{2}J_{\mathrm{PH}}$ = 11 Hz, 1H; IrH). ^{31}P NMR (acetone-d_6, 161.9 MHz, 20 °C): δ 60.67 (m). ^{19}F NMR (acetone-d_6, 376.05 MHz, 20 °C): δ −77.21 (s; $\mathrm{PCF_2C}F_3$), −105.7 to −109.1 (overlapping ABX multiplets; $\mathrm{PC}F_2\mathrm{CF_3}$).

Carbonylation Reactions of (dfepe)$_2$IrH. The reaction of **4** with 1 atm of carbon monoxide was monitored by ^{1}H and ^{31}P NMR spectroscopy in acetone-d_6. After 30 min, resonances for **4** were completely replaced by resonances assignable to a 3:2 mixture of (dfepe)(η^1-dfepe)Ir(CO)H (**5**) and (dfepe)Ir(CO)$_2$H (**6**) and free dfepe. The only iridium species observed after 2 h was **6**. **6** was obtained as a yellow viscous oil after all traces of acetone and free dfepe were removed under vacuum. At ambient temperature neat **6** slowly darkened; analytical samples were low in carbon, suggesting that decomposition involves CO loss and cluster formation. Spectral data for **5**: IR (cm^{-1}) 2116; ^{1}H NMR (acetone-d_6, 400 MHz, 22 °C) δ 3.41 (m, PCH_2), −13.40 (q, $^{2}J_{\mathrm{PH}}$ = 21 Hz); ^{31}P NMR (acetone-d_6, 161.9 MHz, 22 °C) δ 59.2 (m), 42.7 (m), 8.5 (m). Spectral data for **6**: IR (acetone, cm^{-1}) 2051, 2009; IR data for neat oil (cm^{-1}) 2061 vs, 2015 vs, 1845 w, 1415 w, 1305 vs, 1228 vs, 1127 vs, 966 s, 877 w, 809 m, 750; ^{1}H NMR (benzene-d_6, 400 MHz, 22 °C) δ 1.66 (m, PCH_2), −10.20 (t, $^{2}J_{\mathrm{PH}}$ = 57 Hz); ^{31}P NMR (benzene-d_6, 161.9 MHz, 22 °C) δ 69.2 (m); ^{19}F NMR (benzene-d_6, 376.05 MHz, 22 °C): δ −77.64 (s, $\mathrm{CF_2C}F_3$), −112.30 (dd, $^{2}J_{\mathrm{FF}}$ = 309 Hz, $^{2}J_{\mathrm{PF}}$ = 73 Hz; $\mathrm{PC}F_2\mathrm{CF_3}$); −113.70 (dd, $^{2}J_{\mathrm{FF}}$ = 309 Hz, $^{2}J_{\mathrm{PF}}$ = 68 Hz; $\mathrm{PC}F_2\mathrm{CF_3}$).

(dfepe)Ir(H)$_2$(MeCN)$_2$(O$_3$SCF$_3$) (7). Method A. One atmosphere of $\mathrm{H_2}$ was admitted to a solution of 0.100 g of **2** in 10 mL of $\mathrm{CH_2Cl_2}$ at ambient temperature. After 14 h, all volatiles were removed, leaving a yellow oil which was insoluble in ether or hydrocarbon solvents. The oily residue was essentially pure (>95%) **7** by ^{1}H NMR.

Method B. A 0.100-g amount of [(dfepe)$_2$IrH$_2$](O$_3$SCF$_3$) was taken up in 20 mL of acetonitrile and stirred at ambient temperature for 1 day. Removal of solvent gave a yellow oil which was identical with that obtained from hydrogenation of **2**. IR ($\mathrm{CHCl_3}$, cm^{-1}): 2329 m, 2301 m, 1298 vs, 1269 s, 1229 vs, 1139 vs, 1030 s, 972 s. ^{1}H NMR ($\mathrm{CD_2Cl_2}$, 269.7 MHz, 20 °C): δ 2.92 (m, 1H; PCH_2), 2.65 (s, 3H; CH_3CN), 2.60 (m, 3H; PCH_2), 2.50 (s, 3H; CH_3CN), −7.31 (br dd, $^{2}J_{\mathrm{PH}}$ = 19, 206 Hz, 1H; IrH (trans to dfepe)), −19.73 (dd, $^{2}J_{\mathrm{PH}}$ = 11, 24 Hz; IrH (trans to MeCN)). ^{31}P NMR ($\mathrm{CD_2Cl_2}$, 161.9 MHz, 20 °C): δ 71.4 (m), 58.8 (m). ^{19}F NMR (acetone-d_6, 376.05 MHz, 20 °C): δ −76.18, −78.00, −78.17, −78.85 (br s; $\mathrm{PCF_2C}F_3$), −78.36 (s; $\mathrm{O_3SC}F_3$), −106.6 to −115 (overlapping ABX multiplets).

[(dfepe)Ir(H)(μ-H)(OTf)]$_2$ (8). One atmosphere of $\mathrm{H_2}$ was admitted to a solution of 0.250 g (0.246 mmol) of **1** in 20 mL of $\mathrm{CH_2Cl}$ at ambient temperature. An immediate bleaching of the solution from red to yellow was observed, and a crystalline yellow solid began to precipitate. After 1 h the precipitate was filtered off and dried under vacuum. The isolated yield of **8** was 0.192 g (86%). Anal. Calcd for $\mathrm{C_{22}H_{12}F_{46}Ir_2P_4O_6S_2}$: C, 14.52; H. 0.66. Found: C, 14.65; H, 0.62. IR (cm^{-1}): 1700 w, br, 1324 s, 1304 s, 1221 vs, 1143 sh, 1126 s, 1017 s, 967 s, 863 w, 805 w, 752 m, 712 m, 630 m. ^{1}H NMR ($\mathrm{CDCl_3}$, 400 MHz, 22 °C): δ 3.21 (m, 4H; PCH_2), 2.88 (m, 4H; PCH_2), −6.43 (br d, $^{2}J_{\mathrm{PH}}$(trans) = 153 Hz), −29.83 (t, $^{2}J_{\mathrm{PH}}$(cis) = 6 Hz). ^{31}P NMR ($\mathrm{CDCl_3}$, 161.9 MHz, 22 °C): δ 68.1 (m). ^{19}F NMR ($\mathrm{CDCl_3}$, 376.05 MHz, 22 °C): δ −77.47 (s, $\mathrm{O_3SC}F_3$), −78.24 (s, $\mathrm{CF_2C}F_3$), −112.07 (dd, $^{2}J_{\mathrm{FF}}$ = 322 Hz, $^{2}J_{\mathrm{PF}}$ = 53 Hz; $\mathrm{PC}F_2\mathrm{CF_3}$), −114.66 (dd, $^{2}J_{\mathrm{FF}}$ = 322 Hz, $^{2}J_{\mathrm{PF}}$ = 58 Hz; $\mathrm{PC}F_2\mathrm{CF_3}$).

(dfepe)$_2$Ir$_2$(μ-H)$_2$(H)(μ-O$_3$SCF$_3$) (9). A 0.801-g amount of **1** was treated with $\mathrm{H_2}$ in $\mathrm{CH_2Cl_2}$ as described for **8**. After 1 h, replacing dichloromethane by acetone and cooling the solution to −78 °C yielded after filtering and drying 0.425 g (65%) of bright yellow crystalline **9**. Anal. Calcd for $\mathrm{C_{21}H_{11}F_{43}Ir_2O_3P_4S}$: C, 15.12; H, 0.66. Found: C, 14.90; H, 0.75. IR (cm^{-1}): 1591 w, br, 1324 s, 1304 s, 1222 vs, 1143 sh, 1126 s, 1109 sh, 1015 s, 966 s, 866 w, 806 w, 741 m. ^{1}H NMR (acetone-d_6, 269.7 MHz, 20 °C): δ 3.09 (m, 4H; PCH_2), 2.57 (m, 4H; PCH_2), −5.53 (dm, $^{2}J_{\mathrm{PH}}$(trans) ≈ 120 Hz, 2H; Ir(μ-H)), −27.65 (br t, $^{2}J_{\mathrm{PH}}$(cis) = 13 Hz). ^{31}P NMR (acetone-d_6, 161.9 MHz, 20 °C): δ 85.4 (m, 1P), 80.5 (m, 2P), 58.3 (m, 1P). ^{19}F NMR (acetone-d_6, 376.05 MHz, 20 °C): δ −75.36, −76.81, −77.25, −77.40, −78.04, −78.65 (s; $\mathrm{PCF_2C}F_3$), −105.5 to −117 (overlapping ABX multiplets; $\mathrm{PC}F_2\mathrm{CF_3}$).

Reaction of 9 with NEt$_2$H in CH$_2$Cl$_2$. To a solution of 0.250 g (0.149 mmol) of **9** in $\mathrm{CH_2Cl_2}$ at ambient temperature was added excess $\mathrm{Et_2NH}$ (ca. 10 equiv). Upon addition, the solution initially became dark orange and then quickly faded to light yellow. After 30 min the volatiles were removed and the residue was sublimed at 80 °C (10^{-4} Torr) to give 0.122 g (47%) of lemon yellow (dfepe)Ir(Et$_2$NH)Cl, which has been characterized previously.[12] Monitoring of the reaction by ^{1}H NMR indicated that this reaction was quantitative and complete after 2 h.

Crystallographic Studies. X-ray data were collected on a Siemens R3m/V automated diffractometer system with a dedicated Microvax II computer system and fitted with an LT-2 low-temperature device. The radiation used as Mo Kα monochromatized by a highly ordered graphite crystal. The parameters used during the data collection are summarized in Table I. All computations used the SHELTXTL PLUS (Version 3.4) program library (Siemens Corp., Madison, WI).

Crystal Structure of (dfepe)$_2$IrH (4). Recrystallization of **4** from a hot heptane solution yielded colorless irregular blocks of **4** suitable for study. Orthorhombic unit cell dimensions were derived from a least-squares fit of 50 random reflections (20° ≤ 2θ ≤ 30°). Data were collected at −100 °C using the $2\theta/\theta$ scan technique with a variable scan rate of 4.0–30.0° min^{-1}. Analysis of systematic absences for the total data set indicated that the space group was $P2_12_12_1$. Three standard reflections monitored after every 100 data collected showed no systematic variation. An absorption correction using an empirical ellipsoidal model based on φ scans for seven reflections with 10° ≤ 2θ ≤ 35° did not improve the quality of the structure solution and therefore was not applied to the data.

The structure of **4** was solved using direct methods. All non-hydrogen atoms were located on a series of difference Fourier maps and were refined anisotropically. dfepe ligand hydrogen atom positions were added in ideal calculated positions with d(C–H) = 0.96 Å and with fixed isotropic thermal parameters set at 1.1–1.2 times the isotropic equivalent of the attached carbon atom. Full-matrix least-squares refinement gave an R value of 0.065 (R_w = 0.067) for 3471 data with $I > 2\sigma(I)$. The correct absolute configuration of the molecule was verified using an anomalous dispersion multiplier test.[32] The final difference Fourier map showed residual peaks of 2.3 and −3.2 e/Å^3 closely associated with the iridium center (distance <0.8 Å). The location of the hydride ligand position could not be determined due to substantial uncompensated heavy-atom absorption.

Crystal Structure of (dfepe)$_2$Ir$_2$(H)(μ-H)$_2$(μ-O$_3$SCF$_3$) (9). A pale yellow cube of **9** was grown from acetone solution by slow cooling to −50 °C. Data collection procedures and refinement were carried out as described for **4** and are summarized in Table I. Monoclinic unit cell dimensions were derived from a least-squares fit of 48 random reflections (20° ≤ 2θ ≤ 30°). Analysis of systematic absences for the total data set indicated that the space group was $P2_1/n$; the R value for averaging 553 redundant data was 0.045. Data were corrected for absorption using an empirical ellipsoidal model based on φ scans for 12 reflections with 10° ≤ 2θ ≤ 40°.

The structure of **9** was solved using the SHELXTL PLUS Patterson interpretation program; all non-hydrogen atoms were located on a series of difference Fourier maps. Due to data/parameter restrictions, only the iridium and phosphorus atoms, the bridging triflate, and the dfepe backbone carbons were refined anisotropically. dfepe ligand hydrogen atom positions were added in ideal calculated positions with d(C–H) = 0.96 Å and with fixed

---

[32] Rogers, D. *Acta Crystallogr., Sect. A* **1981**, *37*, 734.

isotropic thermal parameters set at 1.1–1.3 times the isotropic equivalent of the attached carbon atom. Full-matrix least-squares refinement gave an R value of 0.063 (R_w = 0.084) for 3808 data with $I > 2\sigma(I)$. The final difference Fourier map showed a number of residual peaks between 1.00 and 1.76 e/Å^3 associated with the iridium and phosphorus centers, as well as several of the CF_3 groups which exhibited relatively large thermal librational motion. As was the case for 4, the locations of the hydride ligand positions could not be reliably determined.

Acknowledgment. This work has been supported by the National Science Foundation (Grant No. CHE-8912697) and the donors of the Petroleum Research Fund, administered by the American Chemical Society. Johnson Matthey is gratefully acknowledged for a generous loan of iridium trichloride.

Supplementary Material Available: Complete X-ray data collection parameters (Tables S1 and S7), bond distances (Tables S3 and S9), bond angles (Tables S4 and S10), anisotropic thermal parameters (Tables S5 and S11), and hydrogen atom coordinates and isotropic thermal parameters (Tables S6 and S12) for 4 and 9 (16 pages). Ordering information is given on any current masthead page.

OM920628L